Protein lactylation within the nucleus independently predicts the prognosis of non-specific triple-negative breast cancer

ANPING GUI[1], XIAOSHAN CAO[2], FENGJIAO MENG[2], YINGZHI CHEN[2], SHIHUI MA[1] and HONG CHEN[3]

[1]Breast Center, People's Hospital of Zhongshan City, Zhongshan, Guangdong 528400, P.R. China;
[2]Department of Pathology, People's Hospital of Zhongshan City, Zhongshan, Guangdong 528400, P.R. China;
[3]Department of Oncological Surgery, People's Hospital of Zhongshan City, Zhongshan, Guangdong 528400, P.R. China

Received August 7, 2024; Accepted November 5, 2024

DOI: 10.3892/ol.2024.14818

Abstract. Protein lactylation represents a pervasive post-translational modification prevalent in histones and diverse proteins, fostering tumor initiation and progression. Nonetheless, the impact of protein lactylation on the prognosis of non-specific triple-negative breast cancer (TNBC) remains uncertain. In the present study, the pan-lysine lactylation (panKlac) levels in cytoplasmic and nuclear compartments were semi-quantitatively examined using a tissue microarray encompassing 77 non-specific TNBC tissues. The association of the prognosis of patients with the panKlac levels in the cytoplasmic and nuclear compartments or other tumor attributes was assessed using Kaplan-Meier and Cox regression analyses. Furthermore, the molecular pathways involved in the promotional effect of lactylation on cell proliferation were determined through a transcriptomic analysis. The results indicated that the panKlac levels were markedly higher in tumor tissues than in para-tumor mammary regions and showed no significant correlations with various clinicopathological parameters, such as tumor dimension, lymph node involvement or histological grading. Notably, high panKlac levels within the nucleus served as an independent predictor of recurrence-free survival, whereas high cytoplasmic panKlac levels were a protective factor for patient survival. The panKlac levels were also markedly elevated in the TNBC cell line, MDA-MB-231. Additionally, glycolysis inhibition significantly reduced the global panKlac levels and concurrently diminished cell proliferation. According to the comprehensive transcriptomic analysis results, pathways related to ribosomal subunit biosynthesis/assembly and aminoacyl-tRNA biosynthesis were involved in the tumor-promoting mechanisms of lactylation. Further results revealed the oncogenic propensity of tyrosyl-tRNA synthetase 1 (YARS1) and its association with lactate production. Overall, Klac levels within the nucleus are an independent prognostic indicator for patients with non-specific TNBC. It is imperative to delve deeper into the roles and mechanisms of nuclear protein lactylation and YARS1 in non-specific TNBC.

Correspondence to: Dr Hong Chen, Department of Oncological Surgery, People's Hospital of Zhongshan City, 2 Sunwen East Road, Shiqi, Zhongshan, Guangdong 528400, P.R. China
E-mail: chenhong_zsph@163.com

Abbreviations: Klac, lysine lactylation; TNBC, triple-negative breast cancer; RFS, recurrence-free survival; TMA, tissue microarray; HER2, human epidermal growth factor receptor 2

Key words: triple-negative breast cancer, lactylation, prognosis, ribosomal pathways, tyrosyl-tRNA synthetase 1

Introduction

Breast cancer (BRCA) has developed as a preeminent life-threatening disease for women on a global scale as a consequence of its elevated incidence and mortality rates. In 2020, there were >2.3 million new cases and 685,000 deaths associated with breast cancer. It is projected that the numbers will exceed 3 million new cases and 1 million deaths annually by 2040 (1). Although the 5-year survival rate of triple-negative breast cancer (TNBC) has been bolstered by advancements in comprehensive treatments, such as surgery, chemotherapy, radiotherapy and molecular targeting therapy, its prognosis remains suboptimal primarily owing to the absence of discernible molecular targets or biomarkers (2,3). At present, a combined approach involving chemotherapy and immune checkpoint inhibitors has become the mainstream treatment for locally advanced (4) and metastatic TNBC (5). The combination of atezolizumab with chemotherapy has demonstrated an increase in the pathological complete response rate by ~17% (58 vs. 41%) compared with chemotherapy alone (4). Therefore, further research is crucial to achieve a comprehensive understanding of the molecular mechanisms underlying TNBC progression, facilitating the creation of more efficacious treatment approaches for TNBC.

Aerobic glycolysis, a metabolic signature of tumor cells (6), not only drives tumor proliferation (7), metastasis (8) and drug resistance (9), but also intricately mediates host antitumor immunity within the tumor microenvironment (10-12). Lactate can be produced by aerobic glycolysis and accumulated within tumor tissues, the understanding of which has been extended from its origins as a metabolic byproduct to its crucial role in driving tumor progression (13). Notably, intracellular lactate

can induce lactylation modifications on histone lysine residues, therefore affecting the transcription of inflammation-related genes and advancing the transformation of M1 macrophages to M2 macrophages (14).

Several studies have underscored the role of histone lactylation in the epigenetic modulation of gene expression and its prognostic significance in human cancer. For instance, higher levels of pan-lysine lactylation (panKlac) and H3K18 lactylation are linked to poorer overall survival outcomes in colon cancer and foster bevacizumab resistance by hyper-activating rubicon-like autophagy enhancer/Pacer transcription (15). In bladder cancer, H3K18 lactylation boosts the transcription of the oncogenic transcription factors, Y-box binding protein 1 and YY1, contributing to cisplatin resistance (16). In ocular melanoma, H3K18 lactylation is associated with elevations in YTH N6-methyladenosine RNA-binding protein 2 (YTHDF2) transcription and decreases in recurrence-free survival (RFS) (17). Therefore, nuclear protein lactylation in TNBC merits comprehensive investigation.

Transfer RNA (tRNA) ligases refer to a class of enzymes that facilitate the binding of specific amino acids to tRNA molecules during intricate peptide chain synthesis. The notable link between lactate and tRNA ligases remained elusive until recent studies revealed the role of alanyl-tRNA synthetase 1 (AARS1) as a potential lactyltransferase. Specifically, AARS1 was found to exert dual effects of either fostering cell proliferation through the lactylation of Yes-associated transcriptional regulator and TEA domain transcription factor 1 or weakening the tumor-suppressive function of p53 via p53 lactylation (18,19). In this context, lactate can be directly recognized, bound and transported to nuclear substrates by AARS1, catalyzing subsequent lactylation reactions in the nucleus.

The current study aimed to investigate the prognostic significance of protein lactylation in patients with non-specific TNBC. Additionally, the oncogenic role and underlying molecular mechanisms of glycolysis in TNBC cells were examined through transcriptomic and bioinformatics analyses.

Materials and methods

Patients and tissue microarray (TMA). In the present study, samples from 100 patients diagnosed with invasive ductal carcinoma (non-specific) type of TNBC at the early stages (stage I-IIA) according to the eighth edition of the primary tumor, lymph node, and metastasis (TNM) classification of the American Joint Commission of Cancer for breast cancer (20) were collected in the Breast Center, People's Hospital of Zhongshan City (Zhongshan, China) between January 2013 and December 2016. All patients underwent surgery as the primary treatment modality without any prior interventions. Adjuvant chemotherapy was performed following radical resection, comprising 4 cycles of epirubicin and cyclophosphamide followed by 4 cycles of paclitaxel. Ipsilateral axillary lymph nodes were dissected if any lymph node dissemination was indicated on imaging, such as ultrasound or magnetic resonance imaging. Alternatively, sentinel lymph node biopsy was performed to confirm no tumor invasion in the local lymph nodes. If axillary lymph node metastasis was observed, radiotherapy was performed.

Subsequent pathological analysis results further excluded 21 patients from the present study due to insufficient tissue samples, specific invasive types or positive hormone receptor and/or human epidermal growth factor receptor 2 (HER2). To reduce potential confounding factors from different biological behaviors, specific invasive types, including metaplastic, medullary and mucinous carcinomas, were excluded from the study. Hormone receptor was considered positive when ≥1% of tumor cells were stained, with intensity ranged from weak to strong (21). HER2 was considered positive when scored 3+ via immunohistochemistry or 2+/+ via fluorescence *in situ* hybridization amplification according to the 2018 American Society of Clinical Oncology/College of American Pathologists Clinical Practice guidelines (22). Additionally, 2 patients were excluded from the study due to the occurrence of another primary breast or thyroid tumor during follow-up. The workflow of experiments involving patients is delineated in Fig. 1.

Core tissue samples (1.5 mm in diameter) were obtained from paraffin-embedded blocks of 77 patients and 37 corresponding para-tumor tissues were also collected. These samples were re-embedded into a TMA by Shanghai Zhuoli Biotechnology Co., Ltd. All tissues were acquired with the informed consent of the patients. The study protocol was conducted with ethical approval from the Clinical Practice and Experimental Research Ethics Committee of the People's Hospital of Zhongshan City (approval no. K2023-113).

Immunohistochemistry. The TMA was sliced into 0.4-μm slides. Following deparaffinization and rehydration in a series of graded alcohols (100, 95 and 80%), the slides were subjected to antigen retrieval by boiling in 10 mM citrate buffer (pH 6.0) for 5 min in a micro-oven. The slides were then immersed in 5% bovine serum albumin (cat. no. A850222; Macklin Biochemical Technology Co.) in Tris-buffered saline with 0.1% Tween 20 for 30 min at room temperature to block non-specific protein binding, and the tissue sections were incubated with 3% H_2O_2 in methanol for 15 min to quench endogenous peroxidase. The slides were then incubated with anti-L-Lactyllysine rabbit monoclonal antibodies (cat. no. PTM-1401RM; 1:300; PTM Biolabs, Inc.) overnight at 4˚C and then with horseradish peroxidase (HRP)-conjugated goat anti-rabbit secondary antibodies (cat. no. A0208; 1:1,000; Beyotime Institute of Biotechnology) for 30 min at room temperature. HRP signals were detected with 3,3'-diaminobenzidine. The stained slides were viewed by two pathologists and any disagreement was addressed by a third senior pathologist. A minimum of three fields (magnification, x200) were analyzed for each slide. The staining intensity was categorized into four grades ranging from 0 to 3 (absent, weak, moderate and strong), and the percentage of positively stained cancer cells was calculated. H scores were calculated by multiplying the staining intensity with the percentage of positively stained cancer cells (23). The slides were scanned with a light microscope (Hamamatsu Photonics K.K.) and images were analyzed with K viewer software (v1.7.0.29; Konfoong Bioinformation Tech Co., Ltd.).

Cell culture and pharmacological interventions. The human TNBC cell line, MDA-MB-231, and the human normal

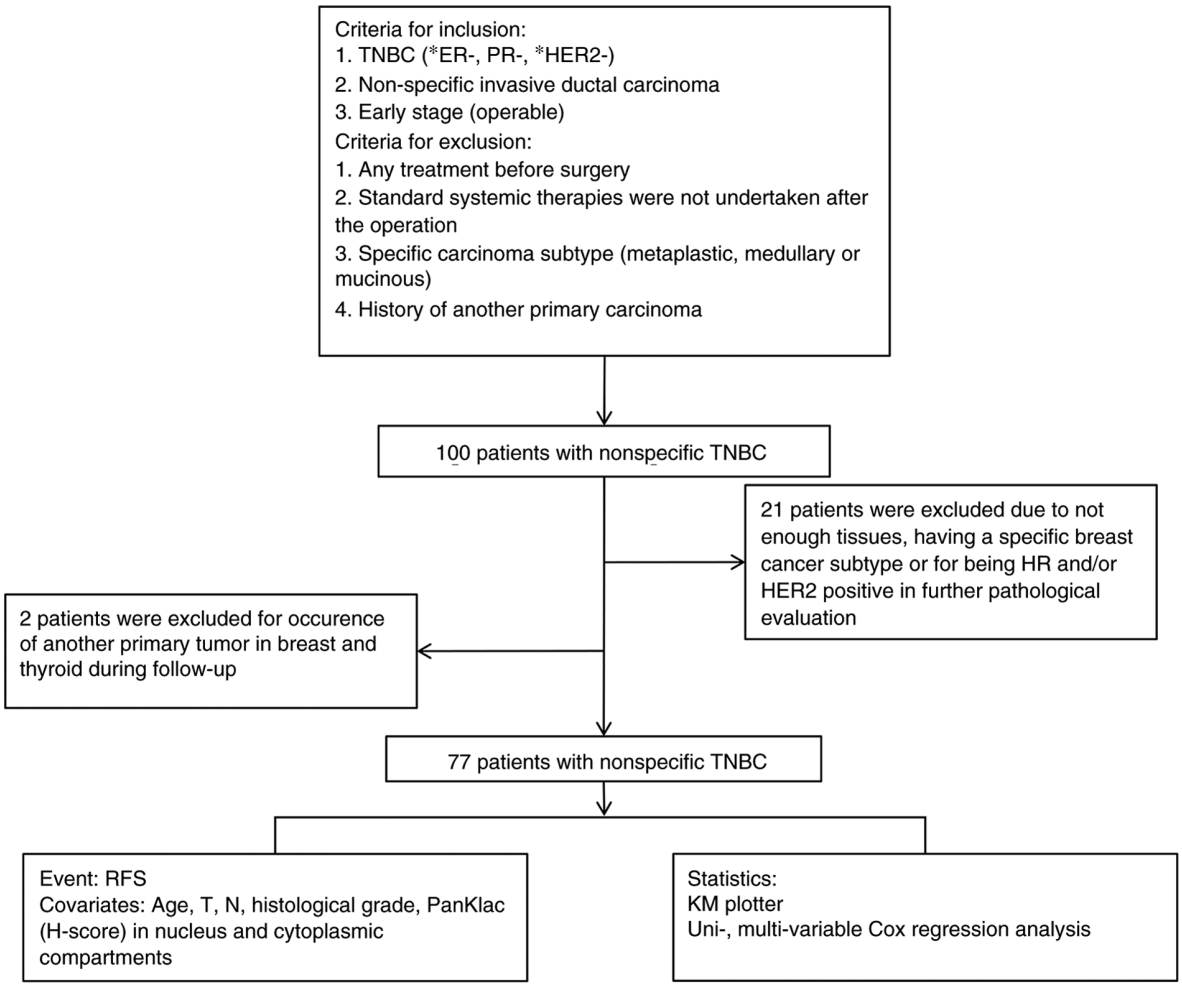

Figure 1. Workflow outlining the selection and study of patients with non-specific TNBC at the early stages. *Negative ER and PR: <1% of cells were stained; Negative HER2: negative-2+ in immunohistochemistry and not amplified in fluorescence *in situ* hybridization. TNBC, triple-negative breast cancer; ER, estrogen receptor; PR, progesterone receptor; HR, hormone receptor; RFS, recurrence-free survival; T, tumor (size); N, lymph node status; panKlac, pan-lysine lactylation.

mammary ductal cell line, MCF-10A, were provided by Procell Life Science & Technology Co., Ltd. The MDA-MB-231 cells were maintained in Roswell Park Memorial Institute-1640 medium (cat. no. 11875500; Gibco; Thermo Fisher Scientific, Inc.) supplemented with 10% fetal bovine serum (FBS; cat. no. SV30208; Hyclone; Cytiva), 100 U/ml penicillin and 100 μg/ml streptomycin (cat. no. EH80010; eLGbio). The MCF-10A cells were maintained in Dulbecco's Modified Eagle Medium/F12 (1:1) supplemented with 10% FBS, 10 μg/ml insulin, 20 ng/ml epidermal growth factor, 100 U/ml penicillin and 100 μg/ml streptomycin (cat. no. CL-0525; Procell Life Science & Technology Co., Ltd.). All cells were cultured in a humidified environment at 37˚C with 5% CO_2. For reverse transcription-quantitative polymerase chain reaction (RT-qPCR), cells were seeded into a 6-well plate ($2x10^5$ cells in 2 ml of medium per well) and treated with 10, 20 or 40 mM oxamate (cat. no. S6871; Selleck Chemicals) in complete growth medium for 24 or 48 h, as indicated in figure legends, at 37˚C. Since the drug was dissolved in ddH2O, an equivalent volume of ddH2O was added to cells in the control group.

Histone protein extraction. Histone proteins were isolated according to the instructions of the EpiQuik Total Histone Extraction Kit (cat. no. OP-0006-100; EpigenTek Group, Inc.) manual before further quantitative analysis by western blotting (WB).

WB. After washing with ice-cold phosphate-buffered saline, cells were lysed in ice-cold Radio-Immunoprecipitation Assay buffers (cat. no. BL504A; Biosharp Life Sciences) containing proteinase inhibitor cocktail (cat. no. 11836170001; Roche Diagnostics) for 30 min. Cell lysates were later sonicated in an ultrasonic cell disruptor (XM-650DT; Shanghai Jingxin Industrial Development Co., Ltd.) at 65 W for 30 sec (2 sec on and 3 sec off) on ice, followed by a 15-min centrifugation at 13,000 x g at 4˚C. Subsequently, sample concentrations were measured with the bicinchoninic acid method (cat. no. A55864; Thermo Fisher Scientific, Inc.). Thereafter, samples (20 or 30 μg of whole cell lysate or 2 μg of extracted histone protein as indicated) were loaded and separated using a 10 or 12% sodium dodecyl sulfate-polyacrylamide gel electrophoresis system and then transferred onto a polyvinylidene fluoride membrane (cat. no. ISEQ00010; MilliporeSigma). After blocking with 5% skim milk for 30 min at room temperature, the membrane was subjected to an overnight incubation at 4˚C with primary antibodies, including

anti-L-Lactyllysine rabbit mAb (cat. no. PTM-1401RM; 1:100; PTM Biolabs, Inc.), anti-L-Lactyl-Histone H3 (Lys14) rabbit mAb (cat. no. PTM-1414RM; 1:100; PTM Biolabs, Inc.), anti-L-Lactyl-Histone H3 (Lys18) Rabbit mAb-ChIP Grade (cat. no. PTM-1427RM; 1:100; PTM Biolabs, Inc.), anti-Histone H3 Rabbit mAb (cat. no. EPR16987; 1:1,000; Abcam) and anti-β-actin mouse mAb (cat. no. 60008-1-Ig; 1:1,000; Proteintech Group, Inc.). The membrane was cut according to the molecular weight markers prior to hybridization with antibodies. Next, the membrane was washed with Tris-buffered saline with 0.1% Tween 20 (pH 7.4) three times (10 min/time) before incubation with HRP-labeled goat anti-mouse (cat. no. A0216) or goat anti-rabbit (cat. no. A0208) secondary antibodies (both 1:1,000; Beyotime Institute of Biotechnology) for 45 min at room temperature. HRP signals were visualized with electrogenerated chemiluminescence reagents (cat. no. EBT002; eLGbio) on the Ephoto™ device [cat. no. L00797c; Mobao (Xiamen) Biotechnology, Co., Ltd.], which was equipped with ePhoto software (v2).

Cell viability assay. For Cell Counting Kit (CCK)-8 assays, cells were seeded into a 96-well plate ($1x10^3$ cells in 100 μl of medium per well). CCK-8 reagents (10 μl; cat. no. CA1210; Beijing Solarbio Science & Technology Co., Ltd.) were added to each well. Following 2 h of cell culture at 37˚C, optical density values at 450 nm were measured with a spectrophotometer. In each experimental setting, wells containing the same medium supplemented with the specified drugs and no cells were utilized as blank controls.

mRNA transcriptomic analysis. The mRNA transcriptomic analysis was conducted by Igenecode Corporation (Beijing Boyun Huakang Gene Technology Co., Ltd.) on the DNBSEQ-T7 sequencing platform. RNA samples were prepared as described in the RT-qPCR section. The clean reads were compared with the human genome using HISAT2 software (v2.2.1; https://daehwankimlab.github.io/hisat2/), followed by quantification of gene expression with StringTie software (v2.1.5; https://github.com/gpertea/stringtie) and the ballgown package (v2.24.0; https://github.com/broadinstitute/ballgown) in R software (v4.3.1; https://www.r-project.org). Principal component analysis (PCA) was performed with the princomp function in R. Differentially expressed genes (DEGs) were screened using the DEseq2 method with the criteria of $|\log2(\text{Fold Change})| \geq 1$ and adjusted $P \leq 0.05$. Subsequent to Gene ontology (GO) annotations with QuickGO (http://www.ebi.ac.uk/QuickGO/), GO enrichment analysis was conducted with the clusterProfiler package in R software. The Kyoto Encyclopedia of Genes and Genomes (KEGG) pathway enrichment analysis was also performed with the clusterProfiler package. Additionally, protein-protein interaction analysis was carried out using the STRING database (https://cn.string-db.org) and the stringDB package. Gene Set Enrichment Analysis (GSEA) was conducted using the GSEA software (http://www.broadinstitute.org/gsea/index.jsp) and the MSigDB database (v7.4).

RT-qPCR. RNA of the MDA-MB-231 cells was isolated as per the protocols of the RNA easy fast animal tissue/cell total RNA extraction kit (cat. no. DP451; Tiangen Biotech Co., Ltd.). The concentration (>100 ng/μl) and purity (A260/280 >2.0) of RNA samples were measured with a nanodrop photometer (NanoDrop 2000; Thermo Fisher Scientific, Inc.). Subsequently, the RNA was kept on ice before being reverse transcribed at 37˚C for 15 min following the manufacturer's instructions using HiScript III RT SuperMix for qPCR (+gDNA wiper; cat. no. R323; Vazyme Biotech Co., Ltd.). The obtained cDNA was quantified with PowerUp SYBR Green Master Mix (cat. no. A25742; Applied Biosystems; Thermo Fisher Scientific, Inc.) on an ABI 7500 Real-Time PCR system (7500; Applied Biosystems; Thermo Fisher Scientific, Inc.). The following thermocycling conditions were used: 50˚C for 2 min and 40 cycles of 95˚C for 2 min, 95˚C for 15 sec and 60˚C for 1 min. The primer specificity was determined with melting curves. The cycling threshold results were determined with the $2^{-\Delta\Delta Cq}$ method (24), with glyceraldehyde-3-phosphate dehydrogenase as the normalization control. Detailed primer sequences are listed in Table I.

Table I. Primer sequences for reverse transcription-quantitative PCR.

Gene symbol	Primer sequences (5' to 3')
GAPDH	F: GCACCGTCAAGGCTGAGAAC
	R: TGGTGAAGACGCCAGTGGA
GCLM	F: CGCACAGCGAGGAGGAGTTT
	R: AATCCAGCTGTGCAACTCCAA
CYP1B1	F: CCTCCTCTTCACCAGGTATCC
	R: TGGTAGCCCAAGACAGAGGT

F, forward; R, reverse; GAPDH, glyceraldehyde-3-phosphate dehydrogenase; GCLM, glutamate-cysteine ligase modifier subunit; CYP1B1, cytochrome P450 family 1 subfamily B member 1.

Database and web-based tool. A web-based tool (https://www.xiantaozi.com/) was used to compare the RNA-sequencing data of paired or unpaired BRCA and normal tissues from The Cancer Genome Atlas (TCGA)-BRCA (https://portal.gdc.cancer.gov). Additionally, the correlation between the expression of YARS1 and other genes was also evaluated using the xiantaozi web-based tool. Furthermore, the disparity in RFS between YARS1-high and YARS1-low groups (split by median value of mRNA expression level by gene chip) was analyzed using the Kaplan-Meier Plotter database (https://kmplot.com/), in which the gene expression data and survival information were downloaded from Gene Expression Omnibus, European Genome-phenome Archive and TCGA (25).

Screening of hub genes. Cytoscape (v3.9.1), which combined public datasets STRING, BioGRID and IntAct (https://cytoscape.org/release_notes_3_9_1.html), was employed to screen the hub genes among the downregulated genes. Betweenness values were acquired using the CytoNCA plugin (https://apps.cytoscape.org/apps/cytonca).

Statistical analysis. The two-tailed Wilcoxon signed rank test was utilized to assess the significance of differences in

panKlac levels between paired tumor and peri-tumor tissue. Unpaired Student's t-test was used to compare the panKlac level in the cytoplasm and nucleus of the tumor tissues, with each from different patients. The association between age and panKlac expression was tested using unpaired Student's t-test. The association between tumor (T) and node (N) stage with panKlac expression was tested using Fisher's exact test. The association between Grade and panKlac expression was tested using the χ^2 test. The Gehan-Breslow-Wilcoxon test was employed for comparing the survival differences between Kaplan-Meier plots. Data from CCK-8 assays and WB were compared (between two groups) with the unpaired Student's t-test. Covariates with significance (P<0.1) in the univariate Cox regression analysis were subsequently included in the multivariate Cox regression analysis to screen the independent indicators of patient survival. YARS1 expression was compared between unpaired normal and tumor samples using the Mann-Whitney U test and between paired normal and tumor specimens with the paired Student's t-test. Spearman correlation analyses were employed to determine expression correlations. Statistical analyses were performed with GraphPad Prism 9.5.1 (Dotmatics), SPSS Statistics 27 (IBM Corp.) or the xiantaozi web-based tool. P<0.05 was considered to indicate a statistically significant difference.

Results

Characteristics of patients. The clinicopathological information of the included patients is listed in Table II. Patients were all female, aged from 33 to 77, with a mean age of 50.44 years. Almost 90% of the patients had a tumor size of T1 or T2 and 9.1% of the patients had a tumor size of T3 or T4. Additionally, 85% of the patients were at N0 or N1, while the rest of the patients were at N2 or N3. There were 61% of the patients at G1 or G2 grades. The follow-up period, which was the interval from the surgery date to disease relapse or loss to follow-up, ranged from 0 to 10.3 years, with a median time of 4.2 years. The H scores of panKlac levels in the cytoplasm and nucleus of tumor and para-tumor mammary tissues are also listed in Table I. The median value was utilized to stratify PanKlac levels in the cytoplasm and nucleus.

panKlac levels are upregulated in the tumor tissues of patients with non-specific TNBC. The representative panKlac immunohistochemistry images are presented in Fig. 2A. Notably, the panKlac levels were significantly higher in tumor tissues than in para-tumor mammary tissues, both in the nucleus (P=0.0175) and cytoplasm (P=0.0038) (Fig. 2B). In the tumor samples, the distribution of the panKlac levels was similar between the cytoplasm and nucleus (P>0.05; Fig. 2C). Notably, the protein lactylation levels within tumors were not associated with various clinicopathological parameters such as age, tumor size, lymph node status or histological grade (Table III).

Association of high panKlac levels in the nucleus with the survival of the cohort of patients with non-specific TNBC. RFS was chosen as the evaluation metric as RFS may be influenced by fewer confounding factors compared with overall survival. All patients with operable TNBC were treated with uniform regimens. However, patients with recurrent disease might have received varying treatments influenced by factors such as economic considerations and the availability of new drugs. RFS displayed associations with clinicopathological features including tumor size (P<0.0001) and lymph node status (P=0.0139) and showed a trend towards an association with panKlac levels in both the nucleus (P=0.0526) and cytoplasm (P=0.0575), but these results were not statistically significant (Fig. 3). In the univariate Cox regression analysis, RFS was linked to T3 or T4 [hazard ratio (HR), 6.918; P=0.034] and N2 (HR, 6.529; P=0.01), and together with N3 (HR, 4.528; P=0.077) and panKlac levels in the nucleus (HR, 3.182; P=0.083) and cytoplasm (HR, 0.297; P=0.069), these variables were passed through to multivariate analysis (Table IV). Through multivariate Cox regression analysis, N2 (HR, 11.171; P=0.010) and elevated panKlac levels in the nucleus (HR, 5.682; P=0.034) were identified as independent prognostic determinants (Table IV).

High levels of lactylation and the proliferation-inhibitory impact of oxamate on BRCA cells. Global lactylation levels were markedly higher in MDA-MB-231 cells compared with the benign mammary epithelial cell line, MCF-10A (Fig. 4A). Moreover, treatment with the lactate dehydrogenase A (LDHA) inhibitor, oxamate, notably diminished the viability (Fig. 4B) and global lactylation levels (Fig. 4C) in MDA-MB-231 cells. Additionally, the lactylation levels of histones (molecular weight of ~15 kDa) were downregulated following oxamate treatment (Fig. 4D). While no decrease in lactylation levels was noted at a concentration of 10 mM, treatment with 20 mM

Table II. Clinicopathological characteristics of the cohort of patients with non-specific triple-negative breast cancer (n=77).

Parameters	Value
Average age (range), years	50.44 (33-77)
T, n (%)	
T1	21 (27.3)
T2	49 (63.6)
T3 or 4	7 (9.1)
N, n (%)	
N0	45 (58.4)
N1	21 (27.3)
N2	6 (7.8)
N3	5 (6.5)
Histological grade, n (%)	
1 or 2	47 (61.0)
3	30 (39.0)
Median duration of follow-up (range), years	4.2 (0-10.3)
Median panKlac, H-score (range)	
Tumor nucleus	90 (0-280)
Tumor cytosol	100 (0-200)
Peri-tumoral nucleus	50 (0-180)
Peri-tumoral cytosol	50 (0-200)

T, tumor (size); N, lymph node status; panKlac, pan-lysine lactylation.

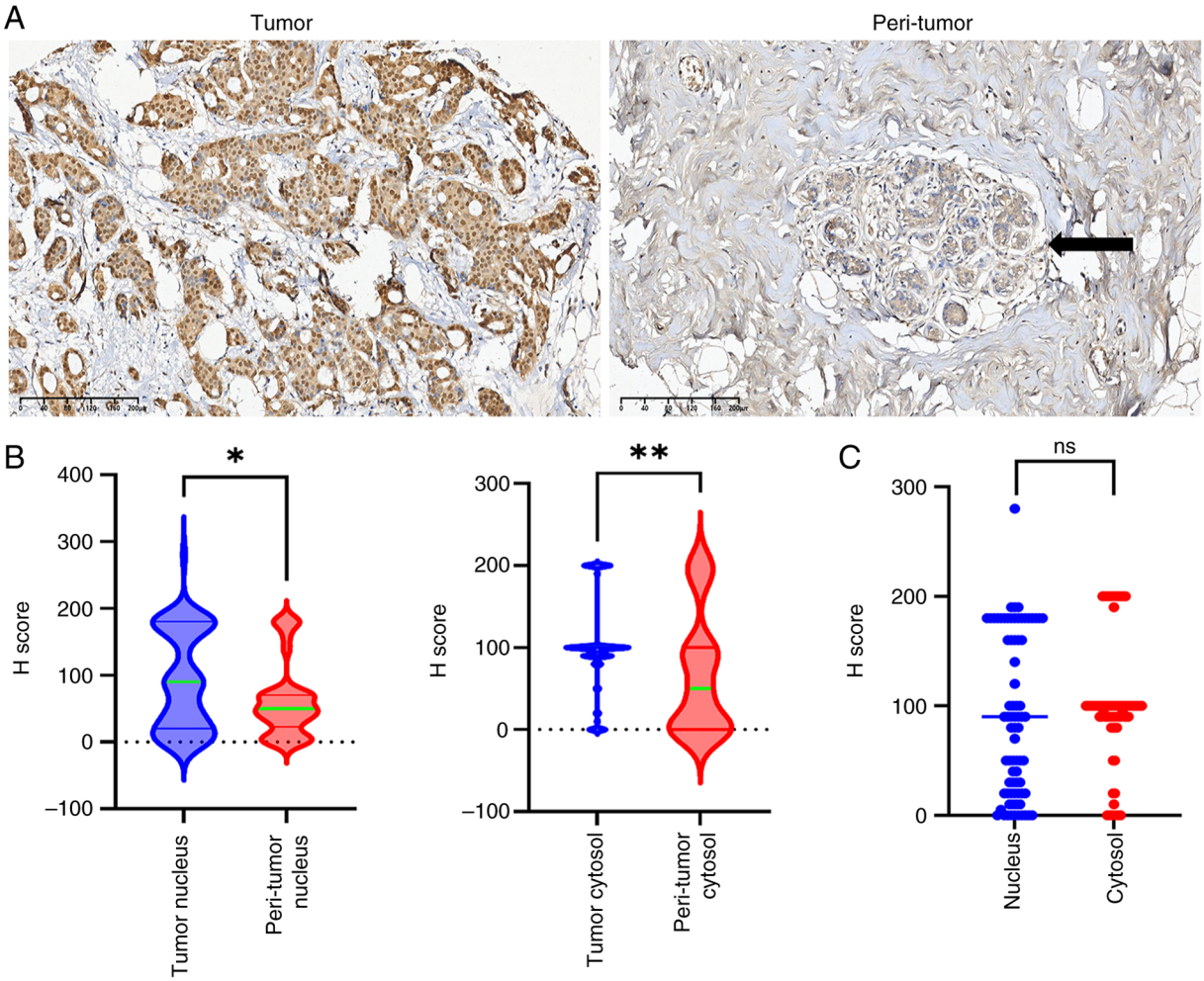

Figure 2. High lysine lactylation levels in breast cancer. (A) Representative images depicting panKlac presence in tumor (left) and para-tumoral mammary tissues (right). The black arrow delineates para-tumor mammary tissues. Scale bar, 200 μm. (B) Comparative assessment of the panKlac staining levels in the nucleus and cytoplasm between tumor and para-tumor mammary tissues, respectively. The results are graphically presented as violin plots, indicating the median, 25 and 75th quantile values. (C) Comparison of the panKlac levels in the cytoplasm and nucleus of the tumor tissues, with each from different patients). Statistical significance was determined with (B) the two-tailed Wilcoxon matched-pairs signed rank test and (C) an unpaired Student's t-test within GraphPad Prism 9.5.1. *P<0.05, **P<0.01. ns, no statistical significance; panKlac, pan-lysine lactylation.

Oxamate significantly induced dose-dependent reductions in lactylation levels of H3K18 and H3K14 residues (Fig. 4E). Overall, the global lactylation status and/or histone lactylation may play a pivotal role in BRCA cell proliferation.

DEGs in the transcriptome. A transcriptomic analysis was conducted to obtain the DEGs between oxamate-treated and untreated cell populations. The PCA results revealed a distinct transcriptomic signature in the oxamate group compared with the control group (Fig. 5A). Following 24 h of oxamate exposure, 265 genes were notably upregulated, while 71 genes were downregulated (Fig. 5B). The fragments per kilobase of transcript per million fragments mapped values of these DEGs were subjected to hierarchical clustering analyses (Fig. 5C). Notably, GO enrichment analysis results demonstrated the involvement of these DEGs in biological processes (BPs) such as 'extracellular matrix organization', 'external encapsulating structure organization' and 'secondary metabolic processes' (Fig. 5D). Furthermore, the KEGG pathway enrichment analysis results indicated the enrichment of these DEGs in pathways including 'Steroid hormone biosynthesis', 'Folate biosynthesis' and 'Metabolism of xenobiotics by cytochrome P450' (Fig. 5E). For validation, RT-qPCR with the RNA samples from the control and oxamate treatment groups was performed, which confirmed the upregulation of cytochrome P450 family 1 subfamily B member 1 and glutamate-cysteine ligase modifier subunit, genes enriched in steroid hormone biosynthesis and ferroptosis pathways, respectively (Fig. 5F).

GSEA results. Compared with the control group, the oxamate-treated group showed reductions in the levels of BP gene sets including ribosomal large subunit biogenesis, translational initiation and ribosomal large subunit assembly (Fig. 6A), cellular compartment gene sets such as ribosomal subunit and large ribosomal subunit (Fig. 6B) and molecular function gene sets associated with the structural constitution of the ribosome (Fig. 6C). Furthermore, the activity of KEGG gene sets encompassing ribosome, DNA replication and aminoacyl-tRNA biosynthesis was lower in the treatment group than in the control group (Fig. 6D). Hallmark gene sets such as Myc, E2F, G2M checkpoint, oxidative phosphorylation, DNA repair and MTORC signaling were

Table III. Association between the Klac level and other clinicopathological factors.

	panKlac nuclear localization			panKlac cytosolic localization		
Parameters	High (n=39)	Low (n=38)	P-value	High (n=44)	Low (n=33)	P-value
Mean age (SD), years	51.28 (9.73)	49.58 (8.689)	0.421	49.41 (9.751)	51.82 (8.383)	0.259
T, n						
T1	14	7		12	9	
T2	21	28		29	20	
T3/4	4	3	0.211	3	4	0.776
N, n						
N0	22	23		27	18	
N1	12	9		12	9	
N2	2	4		4	2	
N3	3	2	0.744	1	4	0.406
Grade, n						
1/2	24	23		26	21	
3	15	15	0.927	18	12	0.686

T, tumor (size); N, lymph node status; panKlac, pan-lysine lactylation.

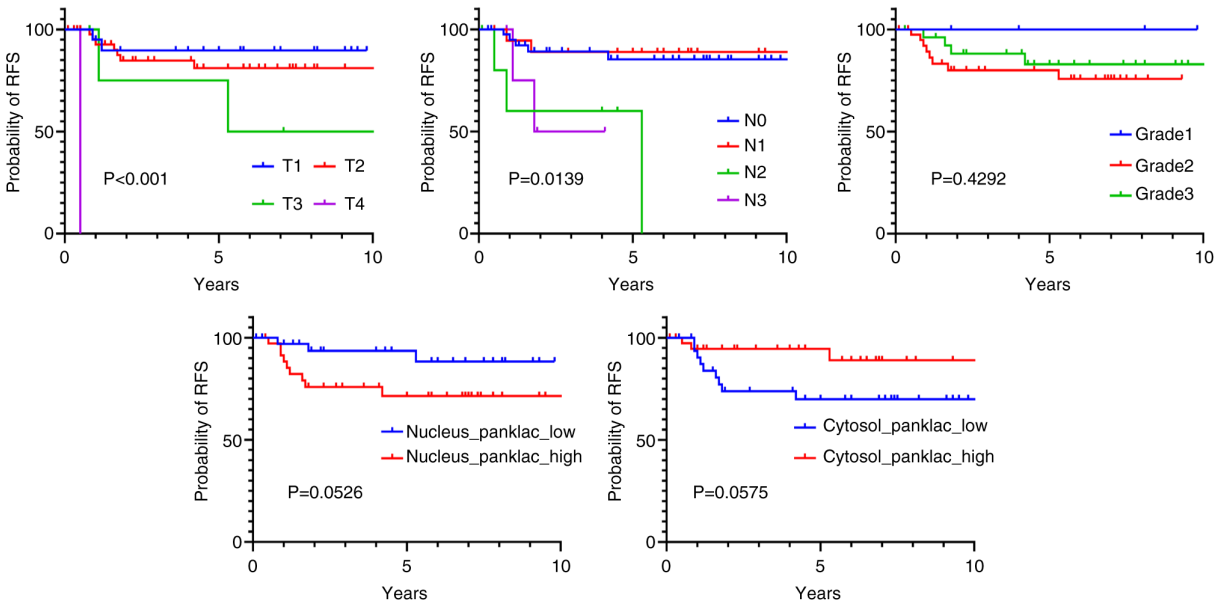

Figure 3. Association between RFS and clinicopathological factors. The clinicopathological factors included T, N, histological grade and panKlac level (as determined by the median H score). Statistical analysis and result visualization were conducted with GraphPad Prism version 9.5.1. RFS, recurrence-free survival; T, tumor (size); N, lymph node status; panKlac, pan-lysine lactylation.

also downregulated in the treatment group vs. the control group (data not shown).

YARS1 as the hub genes. The present study next identified the hub genes among the downregulated DEGs. The top 3 genes, YARS1, coagulation factor XIII A chain and serpina5 were singled out for further analysis due to the high betweenness values (Fig. 7A). Furthermore, the expression correlations of these 3 genes with 3 key glycolysis-related enzymes [LDHA, hexokinase 2 (HK2) and pyruvate kinase M1/2 (PKM)] were analyzed to ascertain their association with glycolysis and protein lactylation. YARS1 exhibited marked correlations with LDHA (ρ=0.434; P<0.001), PKM (ρ=0.427; P<0.001) and HK2 (ρ=0.158; P<0.001) (Fig. 7B), illustrating that YARS1 expression was closely associated with lactate and lactylation. According to TCGA-BRCA data, the RNA expression of YARS1 was significantly higher in BRCA tissues than in normal tissues (Fig. 7C). Moreover, mRNA gene chip data from the Kaplan-Meier Plotter database revealed a significant association between high YARS1 expression and reduced RFS (P=0.00031; HR, 1.2; 95% confidence interval, 1.09-1.33; Fig. 7D).

Table IV. Univariate and multivariate Cox regression analysis of recurrence-free survival.

	Univariate			Multivariate		
Parameters	P-value	HR	95% CI	P-value	HR	95% CI
Age	0.097	1.048	0.991-1.109	0.134	1.058	0.983-1.139
T						
T1						
T2	0.492	1.736	0.361-8.362	0.688	1.429	0.249-8.191
T3/4	0.034	6.918	1.153-41.508	0.218	3.527	0.476-26.157
N						
N0						
N1	0.754	0.769	0.149-3.969	0.466	0.522	0.091-2.993
N2	0.010	6.529	1.552-27.470	0.010	11.171	1.788-69.813
N3	0.077	4.528	0.849-24.162	0.759	1.386	0.173-11.104
Grade						
Grade1/2						
Grade3	0.574	0.709	0.213-2.356	0.729	0.774	0.182-3.298
panKlac level						
Nucleus-panKlac high	0.083	3.182	0.86-11.769	0.034	5.682	1.137-28.394
Cytosol-panKlac high	0.069	0.297	0.08-1.097	0.159	0.356	0.085-1.500

T, tumor (size); N, lymph node status; panKlac, pan-lysine lactylation; HR, hazard ratio; CI, confidence interval.

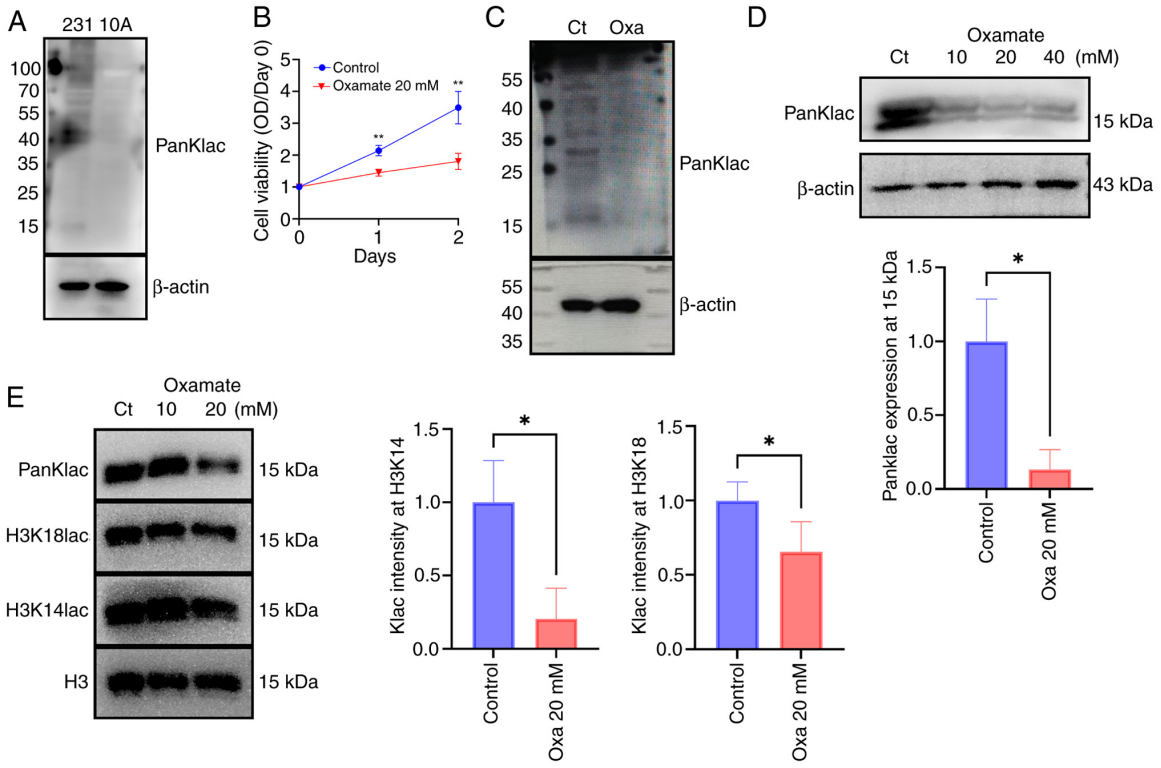

Figure 4. Oxamate decreased Klac levels and inhibited the proliferation of MDA-MB-231 cells. (A) Elevated global Klac levels in the triple-negative breast cancer cell line, MDA-MB-231 compared with the benign mammary epithelial cell line, MCF-10A (loading control: β-actin; whole cell lysate: 20 μg). (B) Significantly repressed cell proliferation after oxamate (20 mM) treatment in MDA-MB-231 cells (blue: control group; red: oxamate group). (C) Significantly decreased global Klac levels after oxamate treatment (loading control: β-actin; whole cell lysate: 20 μg). (D) Significantly decreased Klac levels of histones after oxamate treatment (loading control: β-actin; for Klac: whole cell lysate: 30 μg). The graph is the semi-quantified data of the western blot bands (n=3). (E) Dose-dependent reductions in lactylation levels at H3, H3K14 and H3K18 residues after oxamate treatment (loading control: H3). The analysis was conducted using histone protein extract (2 μg). The graph is the semi-quantified data of the western blot bands (n=3). The membranes were cut in accordance with the molecular weight markers electrophoresed on one or both sides of the membrane before its hybridization with antibodies. All experiments were repeated three times. Statistical significance between the indicated groups in the cell viability and western blotting assays was assessed with the two-tailed unpaired Student's t-test. *P<0.05, **P<0.01. Ct, control group; Oxa, oxamate group; Klac, lysine lactylation.

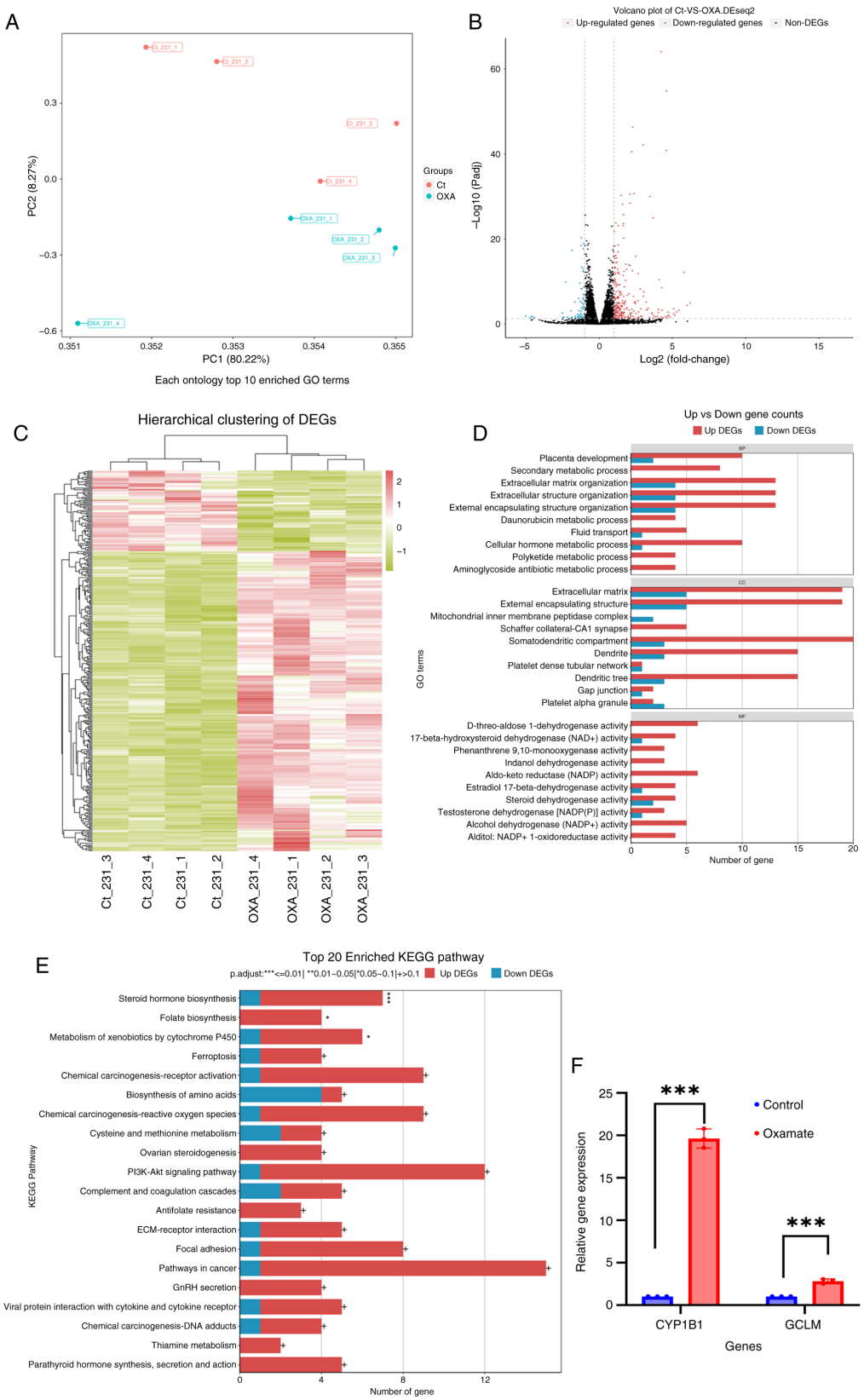

Figure 5. DEG screening and GO/KEGG enrichment between the oxamate and control groups in the transcriptomic analysis. (A) PC analysis of the transcriptome profiles of the oxamate (blue dots) and control (red dots) groups consisting of four biological replicates. (B) Visualization of the DEGs through a volcano plot, where upregulated genes are represented by red dots and downregulated genes are marked by blue dots. Genes with |log2(fold change)|>1 and False Discovery Rate <0.05 were considered DEGs. (C) Hierarchical clustering of the DEGs, with the horizontal axis showing the different samples and the vertical axis representing log10 (fragments per kilobase of transcript per million fragments mapped +1) of gene expression counts, followed by Z-score normalization. (D) GO enrichment analysis of the DEGs, with red bars indicating the upregulated DEGs and blue bars indicating the downregulated DEGs. (E) KEGG enrichment analysis of the DEGs. (F) Upregulation of CYP1B1 and GCLM (two upregulated DEGs) were confirmed using reverse transcription-quantitative PCR. ***P.adjust<0.01, **P.adjust=0.01-0.05, *P.adjust=0.05-0.1; + >0.1.; The experiments were repeated three times. PC, principal component; DEGs, differentially expressed genes; GO, Gene Ontology; KEGG, Kyoto Encyclopedia of Genes and Genomes; Ct, control group; OXA, oxamate group; GCLM, glutamate-cysteine ligase modifier subunit; CYP1B1, cytochrome P450 family 1 subfamily B member 1.

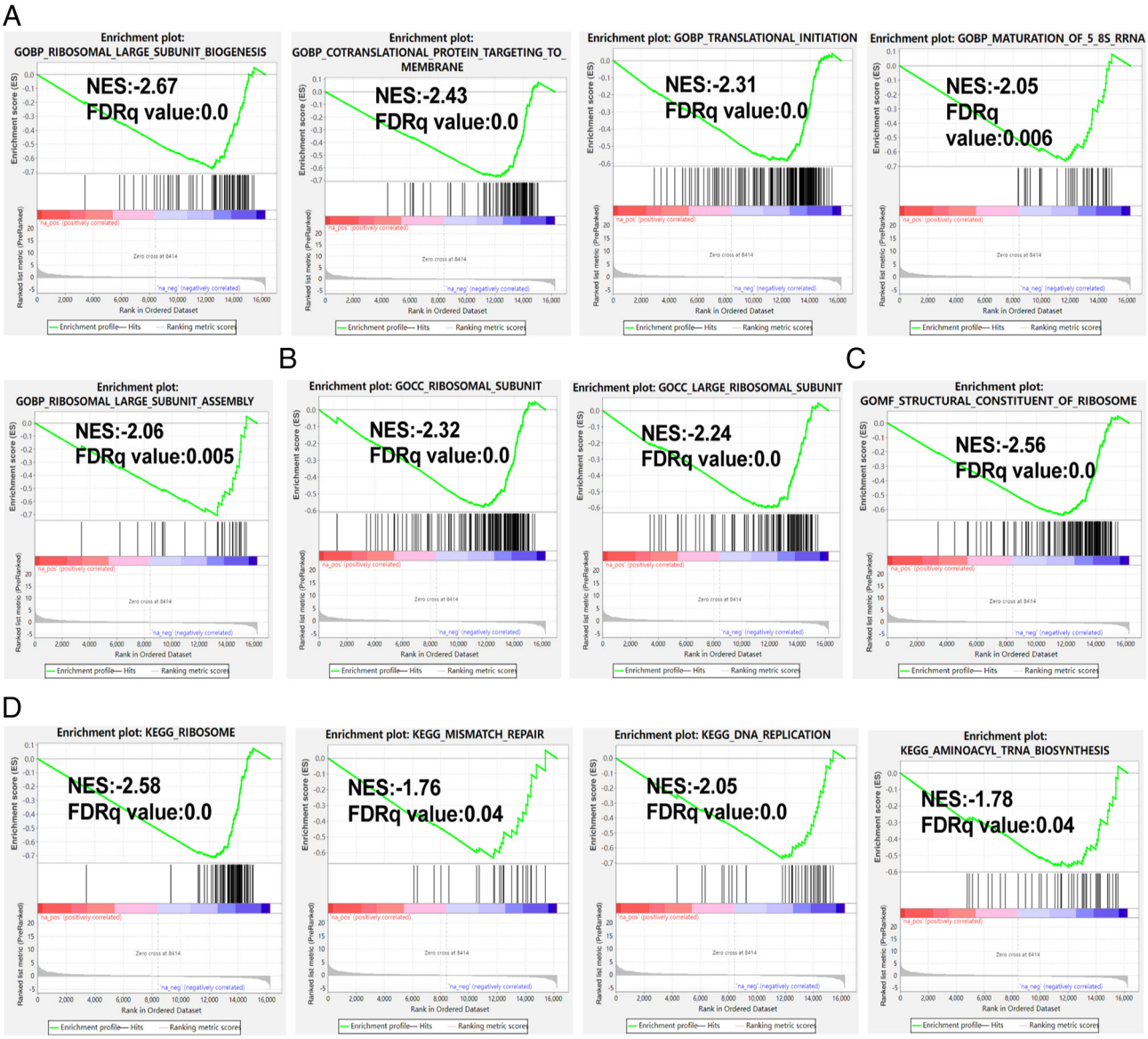

Figure 6. Gene Set Enrichment Analysis of the transcriptomic comparison between the control and oxamate groups. (A) Biological process gene sets downregulated in the treatment group. (B) Cellular compartment gene sets downregulated in the treatment group. (C) Molecular function gene sets downregulated in the treatment group. (D) Kyoto Encyclopedia of Genes and Genomes gene sets downregulated in the treatment group. NES, enrichment scores; FDR, False Discovery Rates.

Discussion

Based on immunohistochemistry and survival analyses, no significant association was found between the panKlac expression level and patient survival using a TMA consisting of various BRCA subtypes (luminal, HER2 amplification and TNBC; cat. no. ZL-Brcsur1801; Shanghai Zhuoli Biotechnology Co., Ltd.) (data not shown). Given that immune surveillance evasion could be a crucial mechanism in TNBC progression (26) and lactylation has been linked to the BRCA immune microenvironment and immunotherapy (27), TNBC was chosen as the focus of the present study. The present study dissected the prognostic significance of global lactylation in non-specific TNBC. To the best of our knowledge, the findings of the present study unveiled for the first time that lactylation levels within the nucleus could independently predict the prognosis of TNBC. However, lactylation levels were not associated with clinicopathological factors such as tumor size, lymph node status and grade. In the *in vitro* experiments, BRCA cells presented with heightened global pan-lactylation levels compared with benign mammary epithelial cells. Additionally, the repression of lactate production mediated by LDHA decreased BRCA cell proliferation. The subsequent transcriptomic analysis results disclosed a potential close correlation between lactylation and the perturbation of ribosomal subunit synthesis and reassembly processes in the nucleus. Furthermore, the results of the present study highlighted the pivotal implication of a tyrosine-tRNA synthetase, YARS1, in both lactylation and BRCA progression.

Until now, limited studies have assessed the prognostic significance of lactylation in BRCA. In a prior lactylome analysis involving 8 paired TNBC samples (tumor and adjacent tissues), upregulation of H4K12 lactylation was determined as an independent prognostic biomarker for TNBC (28). Similarly,

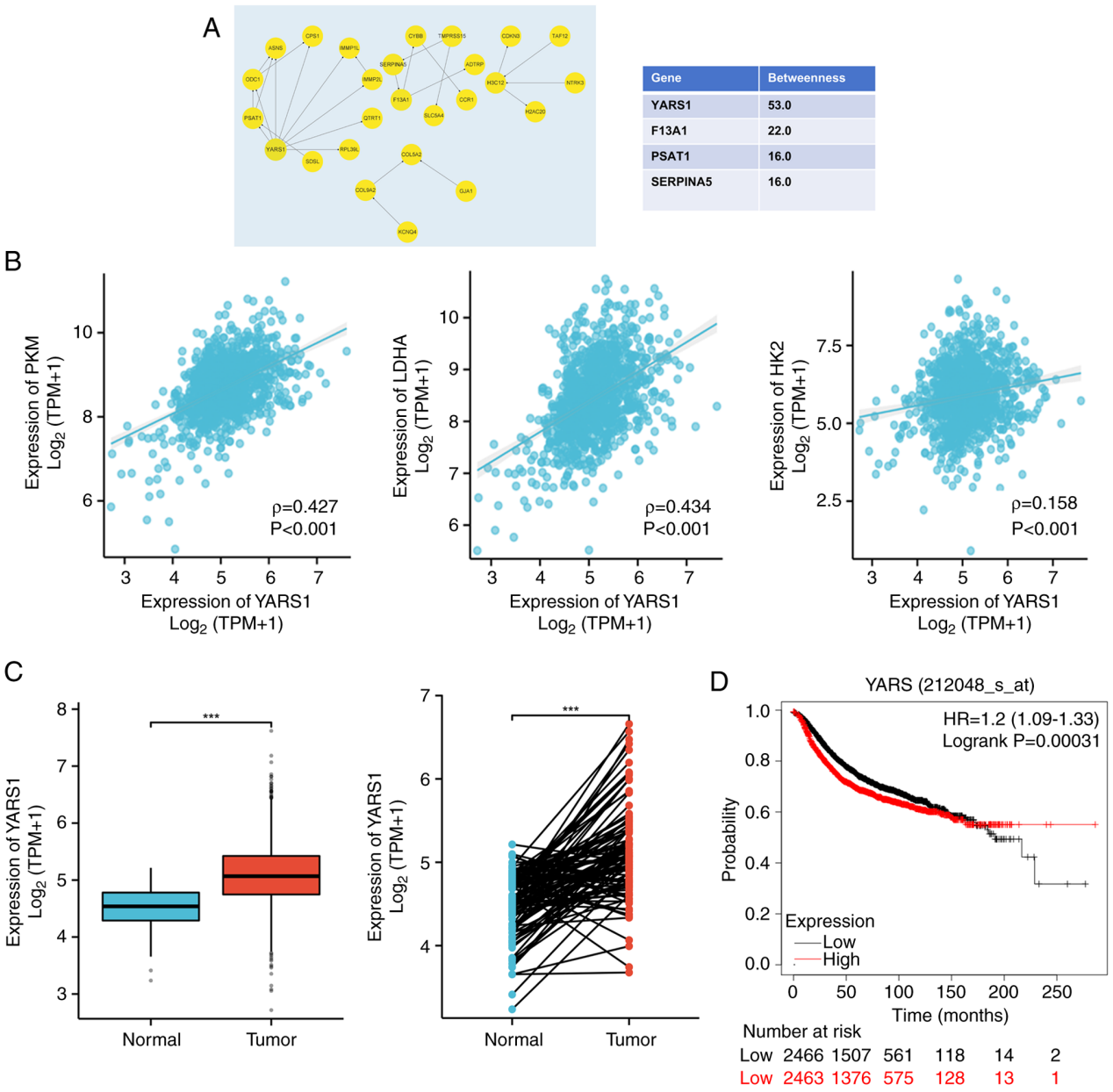

Figure 7. Implications of YARS1 in lactylation and triple-negative breast cancer progression. (A) Visualization of the protein-protein interaction networks involving downregulated genes in the transcriptomic analysis using Cytoscape. (B) Positive correlation of YARS1 expression with various key enzymes associated with lactate production, such as LDHA, PKM and HK2. Expression correlations were determined with the Spearman correlation analysis. (C) Analysis of YARS1 expression in unpaired (left) vs. paired (right) breast cancer samples and normal mammary tissues. The significance of differences in YARS1 expression between unpaired and paired normal and tumor samples was assessed with the Mann-Whitney U test and paired Student's t-test, respectively. These statistical methodologies were chosen in alignment with the attributes of data and implemented with the xiantaozi website-based tool. (D) Association of YARS1 expression with decreased recurrence-free survival in breast cancer according to the Kaplan-Meier Plotter database. ***P<0.01. YARS1, tyrosyl-tRNA synthetase 1; TPM, transcripts per million; LDHA, lactate dehydrogenase A; PKM, pyruvate kinase M1/2; HK2, hexokinase 2.

the findings of the present study revealed that various lysine residues on proteins and histones were universally lactylated in BRCA cells and clinical specimens and that global lactylation within the nucleus was a predictive factor for the prognosis of TNBC. Accordingly, it is of great value to investigate the oncogenic implication of nuclear protein lactylation in TNBC. Prior comprehensive lactylproteomic studies have unveiled numerous lactylation sites in liver carcinoma specimens and oral squamous cell carcinoma cells, with only a handful of sites identified on histones (29,30), signifying that lactylation is a widespread protein modification that extends beyond histones. Certain studies have demonstrated that lactylation may contribute to protein stabilization, therefore potentially exerting oncogenic effects within the nucleus, which may be achieved by boosting oncogene transcription or DNA repair mechanisms in human cancer (31,32). Specifically, in the context of prostate cancer, lactylation stabilizes hypoxia inducible factor 1 subunit α, activating KIAA1199 transcription and ultimately facilitating vasculogenic mimicry in tumor cells (31). Additionally, lactylation enhances the function of MRE11, a pivotal protein participating in homologous recombination that recognizes and repairs damaged DNA in human cancer, and inhibition of MRE11 lactylation impedes DNA repair, thereby inducing the sensitivity of tumor cells to drugs such as cisplatin and poly

(ADP-ribose) polymerase 1 inhibitors (32). These findings corroborate the results of the present study and demonstrate that lactylation levels within the nucleus could serve as a predictor for the prognosis of patients with TNBC.

In the present study, for mechanistic analyses, a comparative transcriptomic analysis was conducted on MDA-MB-231 cells treated with or without a glycolysis inhibitor, which elucidated that DEGs were enriched in gene sets related to ribosomal subunit synthesis/assembly and aminoacyl-tRNA biosynthesis. Hence, further research is warranted to understand the involvement of lactylation in ribosome synthesis and assembly. Additionally, the present study identified YARS1 as a hub gene among the down-regulated DEGs following glycolysis inhibition. Further results showed that YARS1 was positively correlated with key enzymes in glycolysis and lactate production and markedly associated with the prognosis of patients with BRCA. YARS1 has been newly discovered as an oncogene. A previous study revealed the promotional role of YARS1 in the progression of gastric cancer through the PI3K-Akt pathway (33). Furthermore, a more recent study demonstrated that YARS1 is an independent prognostic marker for bladder cancer and potentially affects immune infiltration dynamics and various cancer phenotypes, including senescence, ferroptosis and stemness (34). The present study identified YARS1 as a prognostic marker for TNBC that was closely linked to lactate production and lactylation. Nevertheless, further studies are needed to unveil the intricate mechanisms involved in the regulation of YARS1 expression by lactate and lactylation and the oncogenic mechanism of YARS1 in BRCA.

A limitation of the present study lies in the small sample size of patients with non-specific TNBC. Although RFS displayed a tendency towards correlation with panKlac levels in the nucleus, no statistical significance was observed in the Kaplan-Meier analysis. This lack of significance may be attributed to the small sample size. Nonetheless, it was revealed that increased nuclear panKlac served as an independent marker predictive of an unfavorable prognosis in the multivariate Cox analysis, a comprehensive evaluation that considers various variables. These findings underscore the need for more extensive studies involving a larger sample size to confirm the oncogenic implications of nuclear protein lactylation in TNBC. Furthermore, additional functional experiments and detailed mechanistic investigations are warranted to validate the association between lactylation and YARS1, as the association was only suggested based on bioinformatic analysis in the present study.

In conclusion, it was demonstrated in the present study that lactylation levels in TNBC tissues were higher compared with those in normal tissues, and elevated lactylation levels within the nucleus could be predictive of RFS in patients with TNBC. GSEA and hub gene screening indicated that nuclear lactylation potentially assumes an oncogenic role in TNBC via ribosomal subunit synthesis/assembly and aminoacyl-tRNA biosynthesis pathways. Furthermore, an association was observed between YARS1 and lactylation, highlighting the need for further in-depth mechanistic studies to delve into the intricate relationship among these factors.

Acknowledgements

The authors would like to thank Dr Lan Ting (Department of Advanced Diagnosis Center, People's Hospital of Zhongshan City) for providing technical support throughout the study. The authors would also like to thank Dr Chu Bing (Senior Pathologist, Department of Pathology, People's Hospital of Zhongshan City), for their help when there was a disagreement between our two pathologists. The authors also thank Dr Huang Chensheng (Breast Center, People's Hospital of Zhongshan City) and Dr Zhang Jinhua (Breast Center, People's Hospital of Zhongshan City) for their contributions to the collection of paraffin blocks.

Funding

This study was supported by the Funding of the Key Department of General Surgery (grant no. T2019009) and the Funding of the Graduate Advisor in 2022 (grant no. SG2022YJS0040).

Availability of data and materials

The transcriptome data generated in the present study may be found in the Sequence Read Archive under accession number PRJNA1174689 or at the following URL: https://www.ncbi.nlm.nih.gov/bioproject/PRJNA1174689. Otherwise, the data generated in the present study may be requested from the corresponding author.

Authors' contributions

SM conceptualized the study, while AG devised the research methodology and data collection protocols. AG performed the *in vitro* experimentation and data acquisition. XC performed the immunohistochemistry assays. FM and YC examined the slides and assigned H scores. AG analyzed and elucidated all data to obtain conclusions, construct figures and compose tables. The initial draft of the manuscript was written by AG. SM meticulously evaluated and refined the intellectual depth of the manuscript. HC and SM procured the essential funding for the research endeavor, with HC also involved in conceptualizing the study, and providing supervision and guidance throughout this study. AG, FM and SM confirm the authenticity of all the raw data. All authors have read and approved the final version of the manuscript.

Ethics approval and consent to participate

Tissues were routinely collected from patients during surgery with prior written informed consent from the patients for the use of their tissues and data in research. The study protocol received ethical approval from the Clinical Practice and Experimental Research Ethics Committee of the People's Hospital of Zhongshan City (Zhongshan, China; approval no. K2023-113), followed international and national regulations, and obeyed the Declaration of Helsinki.

Patient consent for publication

Patients provided written informed consent for the publication of their clinical data and images.

Competing interests

The authors declare that they have no competing interests.

References

1. Arnold M, Morgan E, Rumgay H, Mafra A, Singh D, Laversanne M, Vignat J, Gralow JR, Cardoso F, Siesling S and Soerjomataram I: Current and future burden of breast cancer: Global statistics for 2020 and 2040. Breast 66: 15-23, 2022.
2. Derakhshan F and Reis-Filho JS: Pathogenesis of triple-negative breast cancer. Annu Rev Pathol 17: 181-204, 2022.
3. Bianchini G, De Angelis C, Licata L and Gianni L: Treatment landscape of triple-negative breast cancer-expanded options, evolving needs. Nat Rev Clin Oncol 19: 91-113, 2022.
4. Mittendorf EA, Zhang H, Barrios CH, Saji S, Jung KH, Hegg R, Koehler A, Sohn J, Iwata H, Telli ML, *et al*: Neoadjuvant atezolizumab in combination with sequential nab-paclitaxel and anthracycline-based chemotherapy versus placebo and chemotherapy in patients with early-stage triple-negative breast cancer (IMpassion031): A randomised, double-blind, phase 3 trial. Lancet 396: 1090-1100, 2020.
5. Winer EP, Lipatov O, Im SA, Goncalves A, Muñoz-Couselo E, Lee KS, Schmid P, Tamura K, Testa L, Witzel I, *et al*: Pembrolizumab versus investigator-choice chemotherapy for metastatic triple-negative breast cancer (KEYNOTE-119): A randomised, open-label, phase 3 trial. Lancet Oncol 22: 499-511, 2021.
6. Park JH, Pyun WY and Park HW: Cancer metabolism: Phenotype, signaling and therapeutic targets. Cells 9: 2308, 2020.
7. Lunt SY and Vander Heiden MG: Aerobic glycolysis: Meeting the metabolic requirements of cell proliferation. Annu Rev Cell Dev Biol 27: 441-464, 2011.
8. Yang J, Ren B, Yang G, Wang H, Chen G, You L, Zhang T and Zhao Y: The enhancement of glycolysis regulates pancreatic cancer metastasis. Cell Mol Life Sci 77: 305-321, 2020.
9. Chen Y, Zhang J, Zhang M, Song Y, Zhang Y, Fan S, Ren S, Fu L, Zhang N, Hui H and Shen X: Baicalein resensitizes tamoxifen-resistant breast cancer cells by reducing aerobic glycolysis and reversing mitochondrial dysfunction via inhibition of hypoxia-inducible factor-1α. Clin Transl Med 11: e577, 2021.
10. Zhao J, Jin D, Huang M, Ji J, Xu X, Wang F, Zhou L, Bao B, Jiang F, Xu W, *et al*: Glycolysis in the tumor microenvironment: A driver of cancer progression and a promising therapeutic target. Front Cell Dev Biol 12: 1416472, 2024.
11. Yang H, Zou X, Yang S, Zhang A, Li N and Ma Z: Identification of lactylation related model to predict prognostic, tumor infiltrating immunocytes and response of immunotherapy in gastric cancer. Front Immunol 14: 1149989, 2023.
12. Jiao Y, Ji F, Hou L, Lv Y and Zhang J: Lactylation-related gene signature for prognostic prediction and immune infiltration analysis in breast cancer. Heliyon 10: e24777, 2024.
13. Wang T, Ye Z, Li Z, Jing DS, Fan GX, Liu MQ, Zhuo QF, Ji SR, Yu XJ, Xu XW and Qin Y: Lactate-induced protein lactylation: A bridge between epigenetics and metabolic reprogramming in cancer. Cell Prolif 56: e13478, 2023.
14. Zhang D, Tang Z, Huang H, Zhou G, Cui C, Weng Y, Liu W, Kim S, Lee S, Perez-Neut M, *et al*: Metabolic regulation of gene expression by histone lactylation. Nature 574: 575-580, 2019.
15. Li W, Zhou C, Yu L, Hou Z, Liu H, Kong L, Xu Y, He J, Lan J, Ou Q, *et al*: Tumor-derived lactate promotes resistance to bevacizumab treatment by facilitating autophagy enhancer protein RUBCNL expression through histone H3 lysine 18 lactylation (H3K18la) in colorectal cancer. Autophagy 20: 114-130, 2024.
16. Li F, Zhang H, Huang Y, Li D, Zheng Z, Xie K, Cao C, Wang Q, Zhao X, Huang Z, *et al*: Single-cell transcriptome analysis reveals the association between histone lactylation and cisplatin resistance in bladder cancer. Drug Resist Updat 73: 101059, 2024.
17. Yu J, Chai P, Xie M, Ge S, Ruan J, Fan X and Jia R: Histone lactylation drives oncogenesis by facilitating m^6A reader protein YTHDF2 expression in ocular melanoma. Genome Biol 22: 85, 2021.
18. Ju J, Zhang H, Lin M, Yan Z, An L, Cao Z, Geng D, Yue J, Tang Y, Tian L, *et al*: The alanyl-tRNA synthetase AARS1 moonlights as a lactyltransferase to promote YAP signaling in gastric cancer. J Clin Invest 134: e174587, 2024.
19. Zong Z, Xie F, Wang S, Wu X, Zhang Z, Yang B and Zhou F: Alanyl-tRNA synthetase, AARS1, is a lactate sensor and lactyltransferase that lactylates p53 and contributes to tumorigenesis. Cell 187: 2375-2392.e33, 2024.
20. Giuliano AE, Connolly JL, Edge SB, Mittendorf EA, Rugo HS, Solin LJ, Weaver DL, Winchester DJ and Hortobagyi GN: Breast cancer-major changes in the American joint committee on cancer eighth edition cancer staging manual. CA Cancer J Clin 67: 290-303, 2017.
21. Hammond ME, Hayes DF, Dowsett M, Allred DC, Hagerty KL, Badve S, Fitzgibbons PL, Francis G, Goldstein NS, Hayes M, *et al*: American society of clinical oncology/college of American pathologists guideline recommendations for immunohistochemical testing of estrogen and progesterone receptors in breast cancer. J Clin Oncol 28: 2784-2795, 2010.
22. Wolff AC, Hammond MEH, Allison KH, Harvey BE, Mangu PB, Bartlett JMS, Bilous M, Ellis IO, Fitzgibbons P, Hanna W, *et al*: Human epidermal growth factor receptor 2 testing in breast cancer: American society of clinical oncology/college of American pathologists clinical practice guideline focused update. Arch Pathol Lab Med 142: 1364-1382, 2018.
23. Bertozzi S, Londero AP, Viola L, Orsaria M, Bulfoni M, Marzinotto S, Corradetti B, Baccarani U, Cesselli D, Cedolini C and Mariuzzi L: TFEB, SIRT1, CARM1, beclin-1 expression and PITX2 methylation in breast cancer chemoresistance: A retrospective study. BMC Cancer 21: 1118, 2021.
24. Livak KJ and Schmittgen TD: Analysis of relative gene expression data using real-time quantitative PCR and the 2(-Delta Delta C(T)) method. Methods 25: 402-408, 2001.
25. Győrffy B: Survival analysis across the entire transcriptome identifies biomarkers with the highest prognostic power in breast cancer. Comput Struct Biotechnol J 19: 4101-4109, 2021.
26. Knab VM, Gotthardt D, Klein K, Grausenburger R, Heller G, Menzl I, Prinz D, Trifinopoulos J, List J, Fux D, *et al*: Triple-negative breast cancer cells rely on kinase-independent functions of CDK8 to evade NK-cell-mediated tumor surveillance. Cell Death Dis 12: 991, 2021.
27. Deng J and Liao X: Lysine lactylation (Kla) might be a novel therapeutic target for breast cancer. BMC Med Genomics 16: 283, 2023.
28. Cui Z, Li Y, Lin Y, Zheng C, Luo L, Hu D, Chen Y, Xiao Z and Sun Y: Lactylproteome analysis indicates histone H4K12 lactylation as a novel biomarker in triple-negative breast cancer. Front Endocrinol (Lausanne) 15: 1328679, 2024.
29. Yang Z, Yan C, Ma J, Peng P, Ren X, Cai S, Shen X, Wu Y, Zhang S, Wang X, *et al*: Lactylome analysis suggests lactylation-dependent mechanisms of metabolic adaptation in hepatocellular carcinoma. Nat Metab 5: 61-79, 2023.
30. Song F, Hou C, Huang Y, Liang J, Cai H, Tian G, Jiang Y, Wang Z and Hou J: Lactylome analyses suggest systematic lysine-lactylated substrates in oral squamous cell carcinoma under normoxia and hypoxia. Cell Signal 120: 111228, 2024.
31. Luo Y, Yang Z, Yu Y and Zhang P: HIF1α lactylation enhances KIAA1199 transcription to promote angiogenesis and vasculogenic mimicry in prostate cancer. Int J Biol Macromol 222: 2225-2243, 2022.
32. Chen Y, Wu J, Zhai L, Zhang T, Yin H, Gao H, Zhao F, Wang Z, Yang X, Jin M, *et al*: Metabolic regulation of homologous recombination repair by MRE11 lactylation. Cell 187: 294-311.e21, 2024.
33. Zhang C, Lin X, Zhao Q, Wang Y, Jiang F, Ji C, Li Y, Gao J, Li J and Shen L: YARS as an oncogenic protein that promotes gastric cancer progression through activating PI3K-Akt signaling. J Cancer Res Clin Oncol 146: 329-342, 2020.
34. Wang Y, Wang J, Zhang L, He J, Ji B, Wang J, Ding B and Ren M: Unveiling the role of YARS1 in bladder cancer: A prognostic biomarker and therapeutic target. J Cell Mol Med 28: 1-20, 2024.